Multipoint Multichannel Distribution Service at 155 Mbit/sec in 4.6 MHz: an Experimental Prototype Based on Wavefield Modeling

Max Martone, *Member, IEEE*

Abstract— **We report the results of some experimental outdoor field trials which demonstrate the hardware feasibility of fixed broadband wireless radio links with spectral efficiencies in excess of 50 bit/sec/Hz in non line-of-sight environments with frequency selective multipath. Custom hardware has allowed data transmission in the range 60-200 Mbit/sec occupying a bandwidth of 2-4.6 MHz at MMDS frequencies [$\simeq 2.5GHz$]. Moreover, using calibrated antenna collections and sequential spatio-temporal channel estimates in a static environment, we have evaluated transmission with antenna arrays with up to 40 transmit elements and up to 60 receive elements. This last experiment [completed in November 2000] demonstrates the possibility of a 1 Gbit/sec wireless transmission with a raw spectral efficiency of about 208 bit/sec/Hz. While a similar system developed at Bell Labs (known as BLAST) has moved a fundamental step toward the introduction of a technology which may play a key role in future wireless systems, we believe our work extends in many significant ways that initial investigation. First, we overcame the problem of handling a frequency selective channel (as opposed to flat fading): this allowed the study of a larger bandwidth (2-4.6 MHz as opposed to 30 KHz), the experimentation of an outdoor channel and the achievement of significantly higher data rates [of interest in fixed wireless broadband applications]. Second, we have made a conscious effort to design a system where low-cost RF front-ends especially targeted to multiantenna systems could be used. We also introduce a new modeling methodology inspired by basic physics which gives a different and practical perspective to the spatio-temporal transmission problem.**

I. Background

Broadband connectivity has been considered the future of the telecommunications industry for decades and it typically refers to those data services operating at data rates in excess of 1.544 Mbit/sec (known as T-1 rate). While the theoretical foundations of high data rate digital communications are appearently well-known, there has not been any practical solution to implement the massive amount of signal processing required to operate reliably over the poor quality "last-mile" channel. The principal obstacle to mass deployment of broadband data services is without any doubt cost. The wireless terrestrial transmission media presents probably the most difficult challenges. Several types of solutions are being proposed and initially deployed. The Multipoint Multichannel Distribution Service (MMDS) uses microwave transmission at frequency approximately around 2.5 GHz. It is currently envisioned by the wireless communication industry that the MMDS system can broadcast video, voice and data, allowing for interactive communications. MMDS offers a maximum of 33 analog video channels in about 500 MHz and a cell radius approximately 25 to 30 miles. Given the evolution of digital systems, MMDS could provide 2-way connectivity and transport to the transmission nodes enabling ATM or SONET networks. One of the drawbacks of the system is that MMDS relies on traditional high capacity microwave technology which requires Line of Sight transmission and the development of high-performance RF [Radio Frequency] circuitry. This last factor has a dramatic impact on the cost of the Customer Premises Equipment and appears to preclude the successful application of the idea to the residential market. In the United States there are several independent industry efforts that have attacked the problem of high data rate in Non Line of Sight (NLOS) at MMDS frequencies. Members of the Broadband Wireless Internet Forum (BWIF) are committed to sponsor the availability of interoperable solutions based on Coded OFDM (Orthogonal Frequency Division Multiplexing) technology, inspired to the DVB (Digital Video Broadcast) European standard [2]. Products are available now for point to point radio links where the data rate is up to about 25 Mbit/sec in 6 MHz. The use of 2 antennas is exploited only for traditional diversity gain at the receiver.

The Wireless DSL Consortium is fundamentally competing for the same market. The consortium of companies part of Wireless DSL share the goal of providing timely multivendor solutions for the 2 to 4 GHz Point-to-Multipoint Broadband Wireless Access market. To accomplish that goal, the Consortium will pursue a standard based on a physical layer that is a multi-carrier based technology augmented by a system incorporating smart antennas to enable full NLOS operation, otherwise known as MIMO-OFDM (multiple-in multiple-out orthogonal frequency division multiplexing).

Multicarrier systems of the OFDM-type perform a frequency domain decomposition of a channel characterized by frequency selective distorsion in a multitude of subchannels that are affected by frequency flat distorsion. The distorsion in each independent subchannel can then be com-

The author is with WJ Communications, Inc. San Jose, CA 95134, email: max.martone@wj.com.

pensated by simple gain and phase adjustements, somehow overcoming the need of one of the most complex components of a digital modem: the equalizer. On the other hand, coding and transmission power assignments can be applied across the subchannels in a way that resembles the Shannon water pouring argument. As the bandwidth of the subchannels is made sufficiently small one can `in principle` asymptotically reach the channel capacity. This is a relatively old idea which attracted a significant interest in recent years. What is typically neglected in the evaluation of OFDM is that an expensive implementation of the analog RF front-end is extremely critical to the asymptotic behavior of multicarrier transmission. Multicarrier signals, in fact, exhibit extreme vulnerability to distorsions induced by RF electronics. So while able to cope at baseband with channel time dispersions quite effectively (in terms of computational complexity), multicarrier techniques require an increased cost at the RF subsystem level. This is in opposite direction with respect to single-carrier modulations with traditional time-domain equalization. In other words single-carrier schemes appear to be more demanding in terms of DSP resources but the RF front-ends require less stringent specifications. This problem is even more evident in Multi-antenna transmission systems. The idea that multiple transmit/receive antennas have a substantial benefit on the achievable data rate in multipath fading environment has attracted remarkable interest in recent years at least in the research community [4], [5], [6]. Since it is possible to expect an increase in data throughput directly proportional to the number of sensors at the antenna arrays without any penalty in power and bandwidth, this technology appears to be a winning solution in many short and long-range wireless communications applications. However the cost increase of the transceiver is proportional to the number of antennas used by the system because the transceivers have multiple RF and DSP processing branches. Ultimately such a dilemma has slowed down many inititatives in industry. At Lucent, a system called BLAST (Bell-Labs Space-Time Architecture) was developed for a non-frequency selective, static (typically indoor) environment with 30 KHz bandwidth [3]. Despite the undeniable value of that first study it is not difficult to see the restricted applicability of the investigation. While the BLAST group has moved a fundamental step toward the introduction of a technology which may play a key role in future wireless systems, we believe our work extends in many significant ways that initial investigation. First, we overcame the problem of handling a frequency selective channel (as opposed to flat fading): this allowed the study of a larger bandwidth (2-4.6 MHz as opposed to 30 KHz), the experimentation of an outdoor channel and the achievement of significantly higher data rates [of interest in fixed wireless broadband applications]. Second, we have made a conscious effort to design a system where low-cost RF front-ends especially targeted to multiantenna systems could be used. In this paper we describe and discuss the results of the experimental outdoor field trials which have demonstrated the hardware feasibility of fixed broadband wireless radio links with spectral efficiencies in excess of 50 bit/sec/Hz in severe multipath environments. Wireless data transmission in the range 60-200 Mbit/sec occupying a bandwidth of 2-4.6 MHz at 2.5 GHz is achieved. We also introduce a new modeling methodology inspired by basic theoretical physics which gives a different and practical perspective to the spatio-temporal transmission problem and as a byproduct a new class of methodologies which we have defined STREAM$_{TM}$ (Spatial Transmission with Radio Enhanced Adaptive Modulation).

The paper is organized as follows. In Section II we describe the problem of communicating in space-time by means of wavefield modeling. In Section III we describe how wavefields can be effectively represented, while in Section IV we briefly detail a possible detection strategy. Section V focuses on the hardware description and the presentation of the experimental results.

II. Spatio-Temporal Wavefield Modeling

In the context of spatio-temporal processing one is typically interested in wavefields $e(t,\mathbf{r})$ propagating according to the wave equation

$$\left(\nabla^2 - \frac{1}{c^2}\frac{\partial^2}{\partial t^2}\right) e(t,\mathbf{r}) = 0 \tag{1}$$

where c is the velocity of propagation of the medium, $\mathbf{r}$ identifies the spatial location (2-D [$\mathbf{r} = (r,\phi)$] or 3-D [$\mathbf{r} = (r,\phi,\theta)$]) of the propagating wave, t identifies the temporal location of the propagating wave. Assuming that the wavefield has a Fourier representation $e(t,\mathbf{r}) = \int d\omega E(\omega,\mathbf{r}) e^{j\omega t}$, each Fourier component satisfies the source-free Helmholtz equation [1]

$$\left(\nabla^2 + \mathcal{K}^2\right) E(\omega,\mathbf{r}) = 0, \tag{2}$$

where $\mathcal{K} = \frac{\omega}{c}$ is the wavenumber associated with c. In particular we are interested in wavefields generated by linear space-time models expressed as

$$s(t,\mathbf{r}) = \int_T \int_\Gamma h(t,\tau,\mathbf{r},\mathbf{r}') x(\tau,\mathbf{r}') d\mathbf{r}' d\tau \tag{3}$$

where $h(t,\tau,\mathbf{r},\mathbf{r}')$ is the time-variant/space-variant wavefield response of the channel (assumed space-time selective), T is the time interval of interest and , is the spatial volume of interest. Observe that $\mathbf{r}$ is a 3-D or 2-D parametrization of the spatial domain. Roughly speaking $h(t,\tau,\mathbf{r},\mathbf{r}')$ describes the space-time response of the system to an impulse generated at time t [as measured at delay τ] and spatial location $\mathbf{r}'$ [as measured at location $\mathbf{r}$]. If the

channel is time-invariant [$h(t,\tau,\mathbf{r},\mathbf{r}') = h(t-\tau,\mathbf{r},\mathbf{r}')$] we obtain a simple model for the wavefield of interest

$$S(\omega,\mathbf{r}) = \int_\Gamma H(\omega,\mathbf{r},\mathbf{r}')X(\omega,\mathbf{r}')d\mathbf{r}', \tag{4}$$

where $x(t,\mathbf{r}) = \int d\omega X(\omega,\mathbf{r},\mathbf{r}')e^{j\omega t}$, $h(t,\mathbf{r},\mathbf{r}') = \int d\omega H(\omega,\mathbf{r},\mathbf{r}')e^{j\omega t}$.

Assuming a farfield scattering model we can write $H(\omega,\mathbf{r},\mathbf{r}')$ as a a superposition of plane waves

$$H(\omega,\mathbf{r},\mathbf{r}') = \int_\Theta\int_\Theta d\gamma d\gamma' \rho_h(\gamma,\gamma',\omega)e^{j\,\mathbf{r}\cdot\hat{\gamma}\mathcal{K}}e^{j\,\mathbf{r}'\cdot\hat{\gamma}'\mathcal{K}}$$

where:

- Θ is the set of possibles directions of arrival,

$$\Theta = \begin{cases} \phi\in[-\pi,\pi] & \text{if 2-D} \\ \theta\in[0,\pi],\ \phi\in[-\pi,\pi] & \text{if 3-D}\end{cases}$$

- γ and γ' are points in Θ,
- $\hat{\gamma}$ and $\hat{\gamma}'$ are unit vectors pointed in the directions γ and γ',
- $\rho_h(\gamma,\gamma',\omega)$ is a *scattering radiation density.*

$X(\omega,\mathbf{r})$ is expressed as

$$X(\omega,\mathbf{r}) = \sum_{n=1}^{N_{tx}} q_n(\omega)\delta(\mathbf{r}-\mathbf{r}_n)$$

where N_{tx} is the number of elements at the transmit array, $q_n(\omega)$ are the N_{tx} information bearing signals transmitted at the N_{tx} elements of the transmit array, $\mathbf{r}_n$, $n = 1,2,...,N_{tx}$ are the locations of the elements in the transmit array.

Since a plane wave $e^{j\,\mathbf{r}\cdot\hat{\gamma}\mathcal{K}}$ is solution of the Helmoltz equation, $\rho_h(\gamma,\gamma',\omega)$ is an arbitrary complex function fully specified by the spatio-temporal propagation modes of the channel. With the addition of spatially and temporally white noise[1] we have

$$R(\omega,\mathbf{r}) = S(\omega,\mathbf{r}) + N(\omega,\mathbf{r}) \tag{5}$$

For simplicity of notation from now on we will drop the explicit dependence on ω.

We expand the scattering radiation density with a complete and orthogonal (2-dimensional for 2-D propagation or 4-dimensional for 3-D propagation) basis [denoted $f_{n,m}(\gamma,\gamma')$],

$$\rho_h(\gamma,\gamma') = \sum_n\sum_m \psi_{n,m}f_{n,m}(\gamma,\gamma') \tag{6}$$

where $\psi_{n,m}$ are coefficients of the expansion given by

$$\psi_{n,m} = \int_\Theta\int_\Theta d\gamma d\gamma' \rho_h(\gamma,\gamma')f^*_{n,m}(\gamma,\gamma').$$

[1]Noise is also seen as a wavefield $N(\omega,\mathbf{r}) = \int_\Theta d\gamma\rho_n(\gamma,\omega)e^{j\mathbf{r}\cdot\hat{\gamma}\mathcal{K}}$ with its own radiation density $\rho_n(\gamma,\omega)$.

Using (6) we obtain

$$H(\mathbf{r},\mathbf{r}') = \sum_{n,m}\psi_{n,m}\mathcal{H}_{n,m}(\mathbf{r},\mathbf{r}')$$

where

$$\mathcal{H}_{n,m}(\mathbf{r},\mathbf{r}') = \int_\Theta\int_\Theta d\gamma d\gamma' f_{n,m}(\gamma,\gamma')e^{j\,\mathbf{r}\cdot\hat{\gamma}\mathcal{K}}e^{j\,\mathbf{r}'\cdot\hat{\gamma}'\mathcal{K}}.$$

So we can express

$$S(\mathbf{r}) = \sum_{k=1}^{N_{tx}} q_k \sum_{n,m}\psi_{n,m}\mathcal{H}_{n,m}(\mathbf{r},\mathbf{r}_k). \tag{7}$$

Now consider the receive array as a *sampling operator*: from $S(\omega,\mathbf{r})$ it returns a vector $\mathbf{s}(\omega)$ of measurements (the array output)

$$\mathbf{s} = A_R \circ S(\mathbf{r}) \tag{8}$$

where A_R is the *array sampling operator* [a vector valued linear and continuous functional]. Define $\mathbf{a}_{R,n,m,k}$ as the response of the receive array to a wavefield of the form $\mathcal{H}_{n,m}(\mathbf{r},\mathbf{r}_k)$,

$$\mathbf{a}_{R,n,m,k} = A_R \circ \mathcal{H}_{n,m}(\mathbf{r},\mathbf{r}_k).$$

From the linearity of the sampling operator we get

$$\begin{aligned}\mathbf{s} &= A_R\circ S(\mathbf{r}) = \sum_k q_k\sum_{n,m}\psi_{n,m}A_R\circ\mathcal{H}_{n,m}(\mathbf{r},\mathbf{r}_k) \\ &= \sum_k q_k\sum_{n,m}\psi_{n,m}\mathbf{a}_{R,n,m,k} = \sum_k q_k\mathbf{A}_{R,k}\boldsymbol{\Psi},\end{aligned} \tag{9}$$

where $\boldsymbol{\Psi}$ is a vector of coefficients $\psi_{n,m}$ and $\mathbf{A}_{R,k}$ is a matrix of vectors $\mathbf{a}_{R,n,m,k}$ ordered as to properly represent $\sum_{n,m}\psi_{n,m}\mathbf{a}_{R,n,m,k} = \mathbf{A}_{R,k}\boldsymbol{\Psi}$.

Considering the additive noise we obtain the following spatio-temporal model

$$\mathbf{r} = \sum_k q_k\mathbf{A}_{R,k}\boldsymbol{\Psi} + \mathbf{n}. \tag{10}$$

The value of (9) is that it decouples completely the effect of the spatio-temporal channel and the parameters of the transmit/receive array. The vector $\boldsymbol{\Psi}$ fully captures the spatio-temporal channel. An array of isotropic elements in a 2-D spatial representation gives

$$[\mathbf{a}_{R,n,m,k}]_l = \mathcal{H}_{n,m}(\mathbf{r}_l = (r_l,\phi_l),\mathbf{r}_k = (r_k,\phi_k))$$

where $\mathbf{r}_l = (r_l,\phi_l)$ is the location of the lth element in the receive array and $\mathbf{r}_k = (r_k,\phi_k)$ is the location of the kth element in the transmit array.

III. Wavefield Representations Based on Fourier Spatial Expansion

The selection of a basis that parsimoniously represents the radiation density is a critical component of the technology we introduce. One straightforward representation for the "channel" wavefield can be used employing Fourier bases. Consider the 2-D case with

$$f_{n,m}(\gamma,\gamma') = \frac{1}{2\pi} e^{jn\phi} e^{jm\phi'}. \quad (11)$$

The basis set $\mathcal{H}_{n,m}(\mathbf{r},\mathbf{r}')$ can be written [1]

$$\begin{aligned}\mathcal{H}_{n,m}(\mathbf{r}=(r,\phi),\mathbf{r}'=(r',\phi')) &= \int_0^{2\pi}\int_0^{2\pi} d\theta d\theta' \\ & e^{j\mathcal{K}rcos(\theta-\phi)-jn\theta} e^{j\mathcal{K}rcos(\theta'-\phi')-jm\theta'} \\ &= 2\pi j^{n+m} J_n(\mathcal{K}r) J_m(\mathcal{K}r') e^{-j(n\phi+m\phi')}, \quad (12)\end{aligned}$$

where $J_n(\mathcal{K}r)$ is the Bessel function of the first kind. So we obtain

$$\begin{aligned}[\mathbf{a}_{R,n,m,k}]_l &= 2\pi j^{n+m} J_n(\mathcal{K}r_l) J_m(\mathcal{K}r_k) e^{-j(n\phi_l+m\phi_k)} \\ & l=1,2,...,N_{rx}, k=1,2,...,N_{tx}. \quad (13)\end{aligned}$$

It is worth to examine in more detail the relationship of the wavefield model with the traditional model based on manifolfds. Define $\mathbf{a}_R(\gamma)$ and $\mathbf{a}_T(\gamma)$ as the manifolds of the receive and transmit array [in other words $[\mathbf{a}_R(\gamma)]_m$ and $[\mathbf{a}_T(\gamma)]_m$ are the responses of the m-th sensor to a plane wave propagating in the direction γ]. Since

$$\mathbf{a}_R(\gamma) = A_R \circ e^{j\mathcal{K}\mathbf{r}\cdot\hat{\gamma}}$$

and

$$\mathbf{a}_T(\gamma) = A_T \circ e^{j\mathcal{K}\mathbf{r}'\cdot\hat{\gamma}'}$$

where A_R and A_T are the *array sampling operators* [receiver and transmitter respectively], we get

$$\begin{aligned}\mathbf{a}_{R,n,m,k} &= A_R \circ \int_\Theta\int_\Theta d\gamma d\gamma' f_{n,m}(\gamma,\gamma') e^{j\mathbf{r}\cdot\hat{\gamma}\mathcal{K}} e^{j\mathbf{r}_k\cdot\hat{\gamma}'\mathcal{K}} \\ &= \int_\Theta\int_\Theta d\gamma d\gamma' f_{n,m}(\gamma,\gamma') \mathbf{a}_R(\gamma) [\mathbf{a}_T(\gamma')]_k . \quad (14)\end{aligned}$$

This says that $[\mathbf{a}_{R,n,m,k}]_l$ is the Fourier decomposition of the product between the manifolds of the transmit and receive arrays which implies

$$\mathbf{A}_{R,k}\mathbf{w}_{\gamma,\gamma'} = \mathbf{a}_R(\gamma)[\mathbf{a}_T(\gamma')]_k$$

where $\mathbf{w}_{\gamma,\gamma'}$ is a vector organization of the basis functions $f^*_{n,m}(\gamma,\gamma')$.

IV. Detection

For simplicity we consider the uniform linear array configuration, both at the transmitter and at the receiver. We then have

$$[\mathbf{a}_T(\gamma)]_k = e^{j\frac{2\pi}{\lambda}(k-1)d_T sin\theta} \quad k=1,2,...,N_{tx}$$

and

$$[\mathbf{a}_R(\gamma)]_k = e^{j\frac{2\pi}{\lambda}(k-1)d_R sin\theta} \quad k=1,2,...,N_{rx}$$

where d_T and d_R are element separations, respectively at the transmitter and at the receiver arrays and λ is the carrier wavelength. These expressions can be used in (14) and numerical computation of $\mathbf{a}_{R,n,m,k}$ can be performed. The vector $\mathbf{\Psi}(\omega)$ can be truncated to $4N+2$ terms $[\psi_{-N,-N}(\omega),...,\psi_{N,N}(\omega)]^T$. According to the Maximum Likelihood (ML) principle the optimal estimation of the channel parameters can be obtained maximizing

$$\begin{aligned}L_N(\mathbf{\Psi}) &= -\sum_{i=1}^{N_{rx}} \left| [\mathbf{r}]_i - \left[\sum_k q_k \mathbf{A}_{R,k}\mathbf{\Psi}\right]_i \right|^2 \\ &= -||\mathbf{r}-\sum_k q_k \mathbf{A}_{R,k}\mathbf{\Psi}||^2 \\ &= -||\mathbf{r}-\mathbf{S}\mathbf{\Psi}||^2, \quad (15)\end{aligned}$$

which is obtained as $\hat{\mathbf{\Psi}} = \left[\mathbf{S}^H\mathbf{S}\right]^{-1}\mathbf{S}^H\mathbf{r}$. The matrix $\mathbf{S}$ is formed from appropriate training data.

Recall that (10) is function of the frequency. The transmitted signals can be expressed in the time domain as

$$\begin{aligned}\tilde{q}_k(t) &= \sum_l a_k(l) p_k(t-lT_s) \\ &= \sum_l a_k(l) p_{k,l}(t) = \int d\omega q_k(\omega) e^{j\omega t}, \quad (16)\end{aligned}$$

where $a_k(l)$ is a QAM symbol, T_s is the symbol period and $p_k(t)$ a pulse shaping filter. Denoting convolutions as $*$, we have

$$r_i(t) = \sum_{k,l} a_k(l) \sum_{n,m} \tilde{a}_{R,k,n,m,i}(t) * \tilde{\psi}_{n,m}(t) * p_{k,l}(t) + \tilde{n}_i(t)$$

where

$$\tilde{a}_{R,k,n,m,i}(t) = \int d\omega \left[\mathbf{a}_{R,n,m,k}(\omega)\right]_i e^{j\omega t}$$

$r_i(t) = \int d\omega [\mathbf{r}(\omega)]_i e^{j\omega t}$, $\tilde{n}_i(t) = \int d\omega [\mathbf{n}(\omega)]_i e^{j\omega t}$ and $\tilde{\psi}_{n,m}(t) = \int d\omega \psi_{n,m}(\omega) e^{j\omega t}$.

The connection with the commonly assumed MIMO (Multiple Input Multiple Output) model (see for example [8], [9], [11], [10])

$$r_i(t) = \sum_{k=1}^{N_{tx}} \sum_{l=-\infty}^{+\infty} a_k(l) h_{k,i}(t-lT_s) + \tilde{n}_i(t), \quad i=1,...,N_{rx}$$

is evidently obtained as

$$h_{k,i}(t) = \sum_{n,m} \tilde{a}_{R,k,n,m,i}(t) * \tilde{\psi}_{n,m}(t) * p_k(t),$$

or in the frequency domain

$$H_{k,i}(\omega) = \sum_{n,m} a_{R,k,n,m,i}(\omega)\psi_{n,m}(\omega)P_k(\omega),$$

where $p_k(t) = \int d\omega P_k(\omega)e^{j\omega t}$, and $[\mathbf{a}_{R,n,m,k}(\omega)]_i = a_{R,k,n,m,i}(\omega)$. At this point we can look for the optimum MMSE (Minimum Mean Square Error) linear filter $W_{k,i}(\omega)$, whose T_s-spaced sampled output can be expressed as

$$Z_k(\omega) = \sum_{m=-\infty}^{+\infty} \sum_{i=1}^{N_{rx}} W_{k,i}(\omega - 2\pi m/T_s)R_i(\omega - 2\pi m/T_s).$$

We have considered spectrum folding due symbol-rate sampling and used the notation $R_i(\omega) = [\mathbf{r}(\omega)]_i$. The Mean Squared Error is written as

$$MSE_k = T_s \int_{-2\pi/2T_s}^{+2\pi/2T_s} E\left\{|Z_k(\omega) - A_k(\omega)|^2\right\} d\omega,$$

where $A_k(\omega)$ is the Fourier domain representation of $\sum_{m=-\infty}^{+\infty} a_k(m)\delta(t - mT_s)$. For simplicity we assume that there is no excess bandwidth, that is that $P_k(\omega)$ is exactly bandlimited to the Nyquist bandwidth. Since we have

$$H_{k,i}(\omega) = \mathbf{\Psi}(\omega)^T \mathbf{a}_{R,k,i}(\omega)P_k(\omega) = \mathbf{a}_{R,k,i}(\omega)^T \mathbf{\Psi}(\omega)P_k(\omega)$$

we can compact in vector notation

$$\mathbf{H}_k(\omega) = \mathbf{A}_{R,k}(\omega)\mathbf{\Psi}(\omega)P_k(\omega) \tag{17}$$

where

$$\mathbf{H}_k(\omega)^T = [H_{k,1}(\omega), H_{k,2}(\omega), ..., H_{k,N_{rx}}(\omega)].$$

Basically the expression (17) states that $\mathbf{H}_k(\omega)$ is in the subspace spanned by the columns of $\mathbf{A}_{R,k}(\omega)$ which forces the channel vector to lie in the appropriate *a-priori* known subspace: the subspace of the baseband channels generated by plane waves obeying the Helmoltz equation. Compared to unstructured methods [8], [14], this channel parametrization in practice reduces the Mean Square Error of an MMSE detector computed using (17). On the other hand the structure of the model is such that no estimation of angle of arrivals or channel gains is necessary.

The optimum linear MMSE filter is obtained from

$$\begin{aligned} \mathbf{W}_k(\omega) &= [W_{k,1}(\omega), W_{k,2}(\omega), ..., W_{k,N_{rx}}(\omega)]^T \\ &= [\mathbf{R}_H(\omega) + \mathbf{R}_N(\omega)]^{-1} \mathbf{H}_k(\omega) \\ &= \mathbf{R}(\omega)^{-1}\mathbf{A}_{R,k}(\omega)\mathbf{\Psi}(\omega)P_k(\omega) \end{aligned} \tag{18}$$

where $[\mathbf{R}_N(\omega)]_{m,n} = E\{N_n(\omega)N_m^*(\omega)\}$ with $[\mathbf{n}(\omega)]_m = N_m(\omega)$ [2] and

$$\begin{aligned} \mathbf{R}_H(\omega) &= \sum_{k=1}^{N_{tx}} \mathbf{H}_k(\omega)^* \mathbf{H}_k(\omega)^T \\ &= \sum_{k=1}^{N_{tx}} \mathbf{A}_{R,k}(\omega)^* \mathbf{\Psi}(\omega)^* \mathbf{\Psi}(\omega)^T \mathbf{A}_{R,k}(\omega)^T |P_k(\omega)|^2. \end{aligned} \tag{19}$$

The evident problem is that the expansion of $\rho_h(\gamma, \gamma')$ is exact only with an infinite number of components in $\mathbf{\Psi}(\omega)$. Reducing the number of components in $\mathbf{\Psi}(\omega)$ one could trade off bias and variance [7] of the reconstruction error. The MMSE filters can be implemented in the time-domain or in the frequency domain. The preferred implementation used in the experimental prototype is a multirate architecture [13]. The length of the expansion in (17) used in the hardware experiments is $N = 64$.

V. Description of the Hardware Architecture

WJ Communications Inc. (WJCI) has developed a hardware prototype which enabled up to 6-12 transmit antennas and 12-24 receive antennas over a bandwidth up to 5 MHz, with an approximate power at each transmit antenna equal to 25 dBm and at 2.5 GHz. We point out that the BLAST prototype presented in [14] covers approximately 1 % the bandwidth of our prototype and it explores the indoor flat channel at PCS frequencies ($\simeq 1.9GHz$). Fig. 1 and 2 show the architecture of the transceiver.

The transmit and receive antennas (Gain = 7dBi, 70^o azimuthal 3-dB beamwidth, 60^o vertical beamwidth) are connected to the site RF distribution (not shown for simplicity). The Wideband RF Modules (one per antenna, see Fig. 1) are in charge of filtering, amplifying, downconverting and digitizing the RF spectrum of interest. The wideband receiver is designed to be driven from a site RF distribution network and minimizes this interface requiring a single, low gain RF feed per antenna element. High dynamic range amplifiers and mixers are utilized to obtain a large instantaneous dynamic range preserving signal fidelity. The signal as collected by the antenna is filtered and amplified. It is then mixed by a first Local Oscillator and filtered, amplified and mixed down to zero IF (Intermediate Frequency) by an analog quadrature downconverter.

[2] The modification of these expressions for the excess-bandwidth case can be easily determined considering the folded spectra for the channels $H_{k,i}(\omega - 2\pi m/T_s)$ and noise $N_i(\omega - 2\pi m/T_s)$, for $m = -J, -J+1, ..., J$.

$$\mathbf{H}_k(\omega)^T = \left[H_{k,1}(\omega - 2\pi J/T_s), ..., H_{k,N_{rx}}(\omega + 2\pi J/T_s)\right],$$

where $2\pi J/T_s$ is large enough to cover for the excess bandwidth of $P_k(\omega)$.

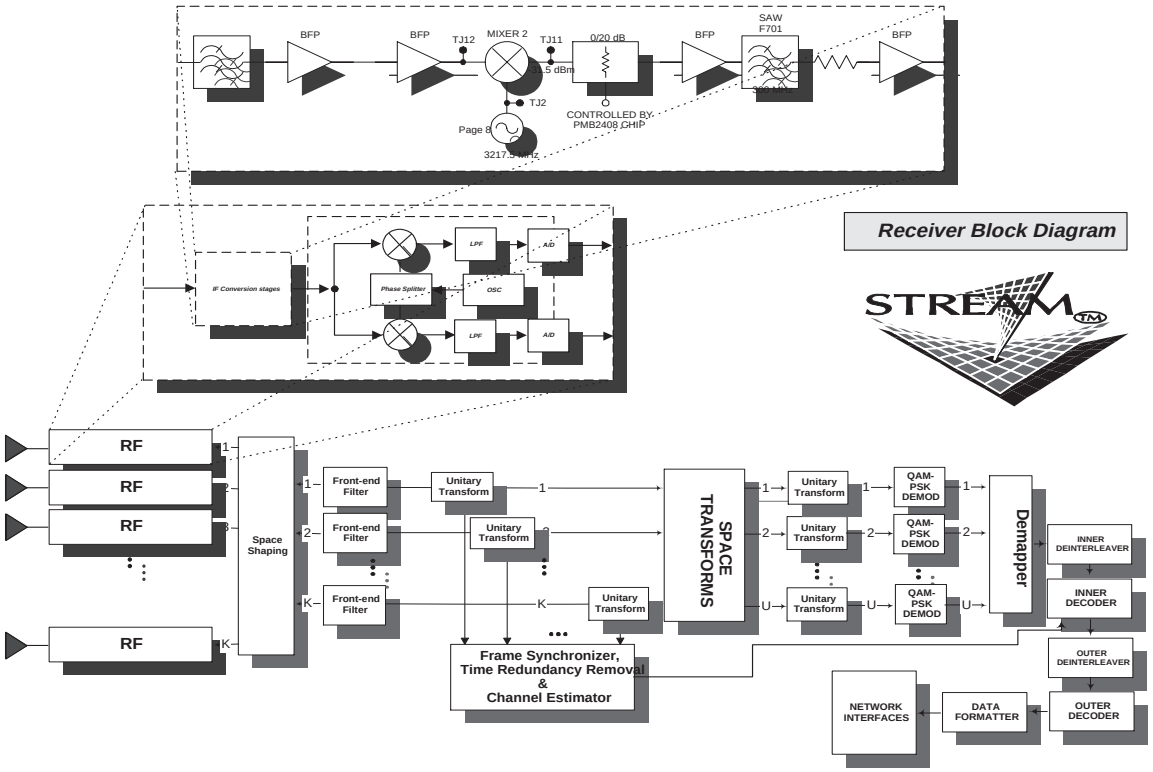

Fig. 1. The Hardware architecture of the Transceiver (receiver section) developed by WJ Communications. DSP data flow is only shown at the functional level.

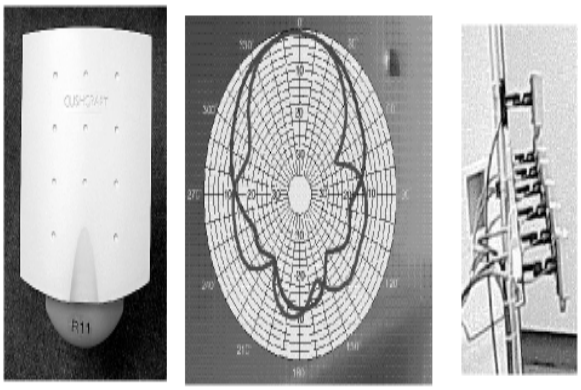

Fig. 3. The antenna used in the prototype and its radiation pattern (horizontal and vertical). On the right the 6 antennas arranged in a linear array. The extra-antenna on top is used for burst synchronization purposes.

Receiver (and Transmitter) architectures can be broadly divided in IF topologies and Zero IF (ZIF) topologies. IF receivers downconvert the wanted signal from its carrier frequency by mixing with a single sinusoidal signal. The signal can be demodulated at the IF or further filtered and downconverted. The main disadvantage of IF receivers is that apart from the wanted signal also an image signal is downconverted to IF. If we define f_{IF} the IF frequency and f_c the carrier frequency, this image frequency is situated[3] at $f_c - 2f_{IF}$. The suppression of the image frequency components is typically done by means of a high frequency filter before downconversion. This filter unfortunately has typically very stringent specifications (high Q and high order even for low f_c/f_{IF} ratios) which makes the overall RF frontend expensive and vulnerable (because made of discrete components that have to be tuned in production). Moreover the integration of these filters into IC is practically impossible. For all these reasons ZIF transceivers (or low-IF transceivers) are typically favored in commercial applications. The ZIF architecture requires the quadrature modulation and demodulation to be performed in the analog domain. It is then important to include in the analysis of the RF system performance I/Q amplitude and phase mismatches caused by the analog implementation of the

[3]Suppose that the wanted signal is $s(t) = cos(\omega_x t + m(t) + \phi)$. At the output of the mixer we have

$$s(t) \cdot sin(\omega_c t - \omega_{IF} t + \psi) = \frac{1}{2} \{sin[\omega_x t + \omega_c t - \omega_{IF} t + \phi + \psi] - sin[\omega_x t - \omega_c t + \omega_{IF} t + \phi - \psi]\} \quad (20)$$

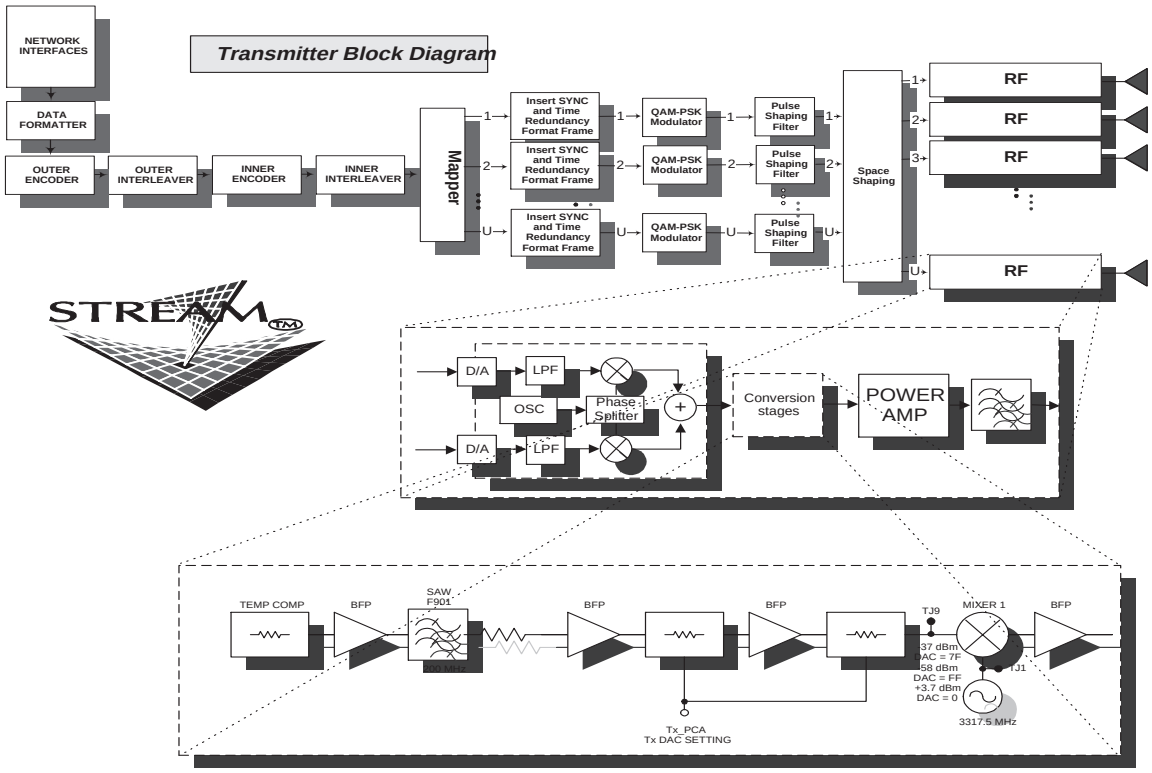

Fig. 2. The Hardware architecture of the Transceiver (transmitter section) developed by WJ Communications. DSP data flow is only shown at the functional level.

baseband shaping filters and phase error of phase splitters. The clock to the analog to digital converters is generated by a frequency source locked to the site frequency reference. The Wideband RF transmitter Module is illustrated in Fig. 2. The samples from the DSP Bus are routed to the the Digital to Analog Converters in complex format and quadrature upconverted to an IF (300 MHz). The RF signal is further filtered, amplified and upconverted. After proper amplification and filtering the signal goes to a power amplifier that is responsible for providing enough RF power to the signal to reach the remote receiver after antenna radiation. The characteristics of the WJCI radio are as follows:

- Noise Figure 5dB,
- 1 dB bandwidth +/-2.05 MHz min,
- 3 dB bandwidth +/-2.5 MHz min,
- Group delay variation: 60 nsec p/p over 1dB bandwidth,
- Phase Noise:
  - -80 dBc at 1KHz,
  - -95 dBc at 10KHz,
  - -120 dBc at 100KHz,
  - -138 dBc at 1 MHz,
- Receiver Dynamic Range: -98 dBm to -20 dBm,
- Reference Stability: +/- 2.5 ppm,
- Transmitter 1dB compression point +27dBm.

The transceivers are locked to a common frequency reference. DSP is shown only at the functional level: in reality the outputs of the A/D and inputs to the D/A are connected to high speed memory modules. Such modules allow back-end processing relaxing the real-time constraint. For the experimental set-up frames are post-processed off-line. The signal processing functions at the transmitter include: a frame formatter, QAM modulators, pulse shaping filters and spatial signal conditioners. The signal processing functions at the receiver include: spatial signal deconditioners, front-end filters, unitary time-domain transforms spatial domain processing, unitary time-domain anti-transforms QAM demodulators, pulse shaping filters. The channel coding strategy is inspired to the concatenated approach. Encoders and interleavers are specified in [2]. Data formatting refers to the organization of the information bitstream in a way that is compatible with the particular application of the communication system. A picture of the transmitter/receiver rack is reported in Fig. 4. It is commonly believed that modem methodologies based on multi-antenna systems have an increase in computational complexity of the baseband processing if compared with traditional single antenna methods. In Fig. 5 we report the complexity of the baseband processing of the proposed Modem technol-

Fig. 4. The transceiver rack front-end for 6 transmit/12 receive antennas.

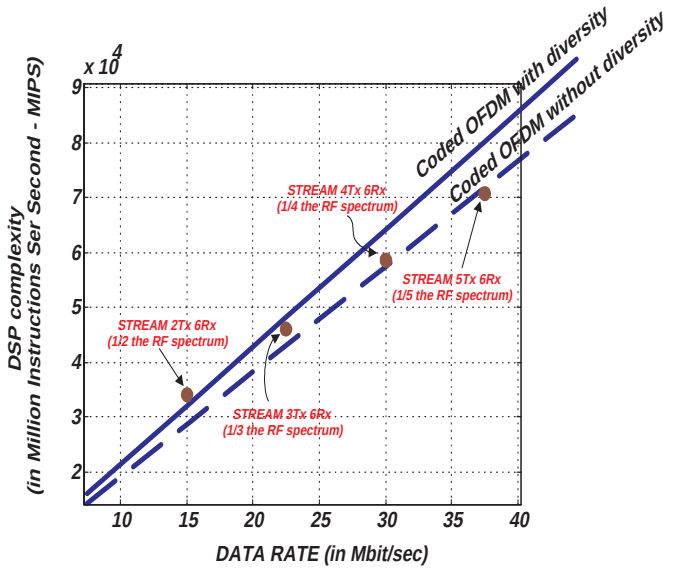

Fig. 5. Complexity of the baseband processing of the proposed Modem technology in terms of MIPS as a function of the deliverable payload data rate. Channel coding is punctured convolutional coding (rate 3/4) and soft-decision decoding for both Coded OFDM (single transmit antenna) and STREAM.

ogy in terms of MIPS (Millions of Instructions per Second) as a function of the deliverable payload data rate. Channel coding is punctured convolutional coding (rate 3/4) and soft-decision decoding for both Coded OFDM (single transmit antenna) of [2] and STREAM$_{TM}$. The striking result is that the DSP complexity of a single antenna Coded OFDM system according to the standard [2] has the same baseband DSP complexity of a multi-antenna STREAM$_{TM}$ modem which delivers the same data rate, while having approximately $1/N_{tx}$ bandwidth occupation.

VI. Experimental Results

The platform used for the hardware trials was completed in July 2000. Integration progress for the hardware modules with relative spectral efficiencies is reported in Fig. 6. The signal modulation employed at each antenna is 64-QAM and the baseband filters $P_k(\omega)$ are raised cosine filters with roll-off equal to 0.15. The Peak to Average Ratio remains within 6-9 dB which makes the technique significantly more advantageous than OFDM. SNR is calculated as described in [14]. A map of the locations used to perform the transmission experiments in the former Watkins-Johnson campus in Palo Alto, California is available on request from max.martone@wj.com. Such an environment is representative of a wireless local loop application with average range equal to 0.5 miles. The delay spread reaches a worst case condition of 2 μsec. The antennas are arranged in a rectangular planar configuration ($\simeq$ 1 wavelength spacing), $6 \times M$, M variable. We also report results for a number of antennas larger than the ones available in hardware using the following methodology. Define M_T positions for the transmit N_{tx}-antenna array $\mathbf{r}_i$ $i = 1, 2, ..., N_{tx}$ and M_R positions for the receive N_{rx}-antenna array $\mathbf{r}'_k$ $k = 1, 2, ..., N_{rx}$. A channel for a $M_T N_{tx} \times M_R N_{rx}$ system [we mean $M_T N_{tx}$ transmitters and $M_R N_{rx}$ receivers] $\mathbf{H}_{M_T N_{tx} \times M_R N_{rx}}(\omega)$ can be thought as composed of channels $\mathbf{H}^{(i,k)}_{N_{tx} \times N_{rx}}(\omega)$ for $N_{tx} \times N_{rx}$ systems, where the transmit array is at some position $\mathbf{r}_i$ and the receive array is at some position $\mathbf{r}'_k$. So the assumption of a reasonably static channel[4] for the $\mathbf{H}_{M_T N_{tx} \times M_R N_{rx}}(\omega)$ allows us to perform the estimation of the channel with only N_{rx} elements at the receiver and N_{tx} elements at the transmitter by estimating (at different times) *smaller* channels $\mathbf{H}^{(i,k)}_{N_{tx} \times N_{rx}}(\omega)$ $i = 1, ..., N_{tx}$ and $k = 1, ..., N_{rx}$. After having performed the $M_T M_R$ channel estimations we compose the *large* channel $\widehat{\mathbf{H}}_{M_T N_{tx} \times M_R N_{rx}}(\omega)$ using $\widehat{\mathbf{H}}^{(i,k)}_{N_{tx} \times N_{rx}}(\omega)$ $i = 1, ..., N_{tx}$ and $k = 1, ..., N_{rx}$. Subsequently we can process QAM data using DSP baseband processing on the channel $\widehat{\mathbf{H}}_{M_T N_{tx} \times M_R N_{rx}}(\omega)$. We have fundamentally exploited the channel time invariance and emulated signal collections in absence of moving objects (most of these collections were performed during night hours). A "1 Gbit/sec" experiment is performed using $M_T = 10$, $N_{tx} = 4$, $M_R = 10$ $N_{rx} = 6$, for a total of 40 transmit antennas and 60 receive antennas. We achieve a raw data rate of 960 Mbit/sec in 4.6 MHz at SNR=30 dB (at this SNR a punctured convolutional coding scheme, rate 5/6 provides $BER < 10^{-6}$). In Fig. 7

[4] The sequential channel measurements are performed coherently by locking oscillators at transmitter and receiver.

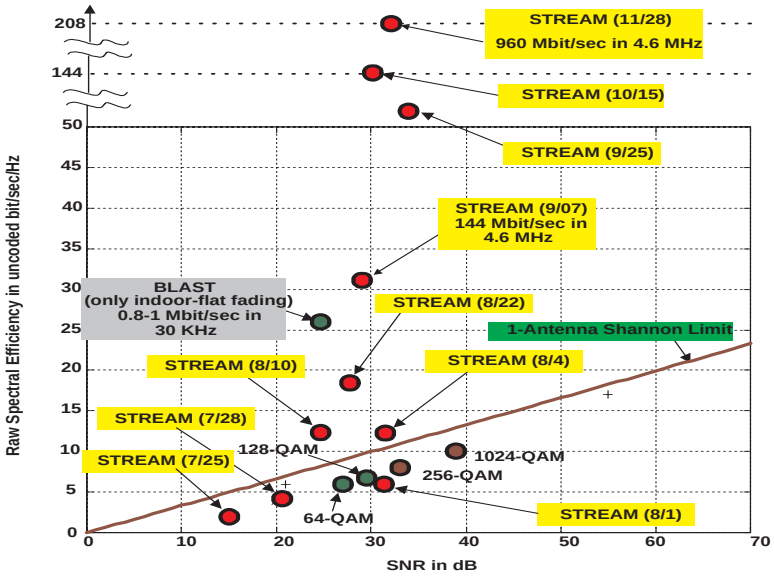

Fig. 6. Progress of achieved raw spectral efficiencies in Non Line of Sight wireless transmissions. The indicated SNRs are relative to a $BER < 10^{-6}$ with an overhead equal to 28 % (channel coding is a punctured convolutional code with rate 5/6 with soft-decision decoding).

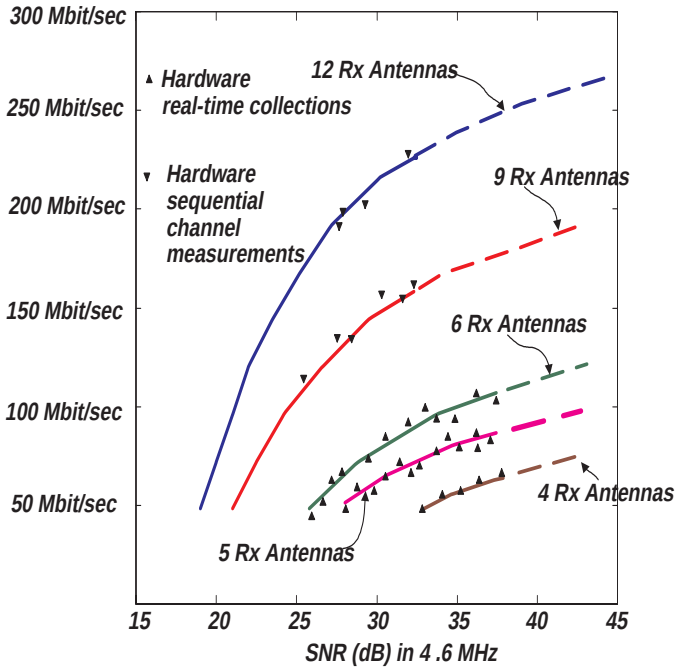

Fig. 8. Bit Error Rate results averaged over different locations in 4.6 MHz. Curves are for convolutionally coded (rate 5/6) 64-QAM.

we show hardware results for a particular NLOS situation. The delay spread is about 1 μsec. In Fig. 8 we summarize the achieved data rates for BER less than 10^{-6} (with a 5/6 punctured convolutional encoder) in 4.6 MHz averaged over different locations. The data rates shown account for 28% overhead due to channel coding and frame overhead for training and time-frequency synchronization.

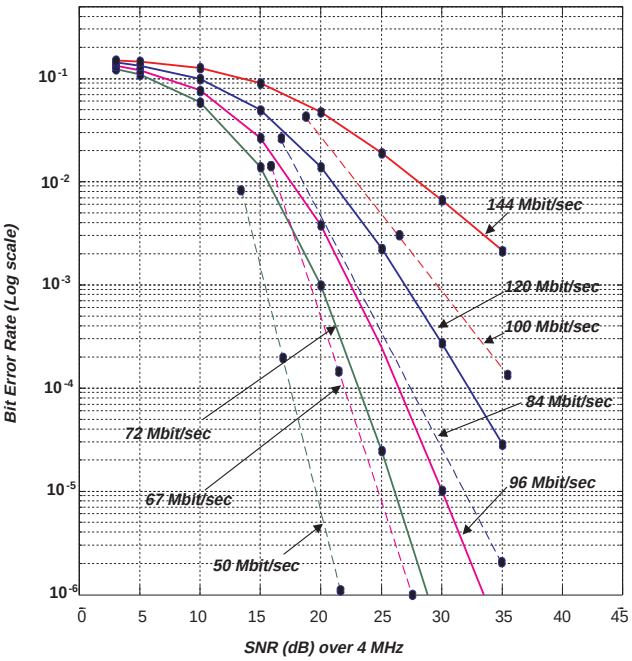

Fig. 7. Bit Error Rate results for outdoor obstructed (non Line of Sight) in 4.6 MHz environment with 3 , 4 and 5 transmit antennas, 6 receive antennas. Dashed curves are for punctured 3/4 convolutionally encoded 64-QAM. Solid curves are for uncoded 64-QAM.

VII. Conclusions

We have described the results of some experimental outdoor field trials which have demonstrated -for the first time- the hardware feasibility of fixed broadband wireless radio links with spectral efficiencies in excess of 50 bit/sec/Hz in severe multipath environments. Wireless data transmission in the range 60-200 Mbit/sec occupying a bandwidth of 2-4.6 MHz at 2.5 GHz was achieved. The significant value of these results is implicitly related to the achievement of incredible spectral efficiencies in arbitrarily severe multipath, non line of sight and with inexpensive RF hardware currently manufactured by WJCI and DSP complexity well within the capability of current state of the art digital technology. Using calibrated antenna collections and sequential spatio-temporal channel estimates in a static environment, we have evaluated transmission with antenna arrays with up to 40 transmit elements and up to 60 receive elements. This last experiment [completed in November 2000] demonstrates the possibility of a 1 Gbit/sec wireless transmission with a raw spectral efficiency of about 208 bit/sec/Hz. While a similar system developed at Bell Labs (known as BLAST) has moved a fundamental step toward the introduction of a technology which may play a key role in future wireless systems, we believe our work extends in many significant ways that initial investigation. First, we overcame the problem of handling a frequency selective channel (as opposed to flat fading): this allowed the study of a larger bandwidth (2-4.6 MHz as opposed to 30 KHz), the experimentation of an outdoor channel and the achievement of significantly higher data rates [of interest in fixed wireless broadband applications]. Second, we have made a conscious effort to design a system where low-cost RF front-ends especially targeted to multiantenna systems could be used.

References

[1] P. M. Morse and H. Feshback, *Methods of Theoretical Physics*, New York: Mac Graw-Hill, 1953, pt I.

[2] "Digital Video Broadcasting (DVB); framing structure, channel coding and modulation for digital terrestrial television (DVB-T)" *European Telecommunications Standard*, ETS-300-744, March 1997.

[3] G. J. Foschini, "Layered space-time architecture for wireless communication in a fading environment when using multi-element antennas," *Bell Labs Tech. J.*, vol. 1, no. 2, pp. 41-59, 1996.

[4] V. Tarrokh, N. Seshadri and A. R. Calderbank, "Space-Time Codes for High Data Rate Wireless Channels Communication: Performance Criterion and Code Construction", *IEEE Transactions on Information Theory* , vol. 44, n. 2, March 1998.

[5] J. Winters, "On the capacity of radio communication systems with diversity in a Rayleigh fading environemt," *IEEE J. Select. Areas Commun.*, vol. SAC-5, pp. 871-878, June 1987.

[6] G. G. Raleigh and J. M. Cioffi, "Spatio-temporal coding for wireless communication," *IEEE Trans. Commun.*, vol. 46, pp. 357-366, Mar. 1998.

[7] L. L. Scharf. *"Statistical Signal Processing"*, Addison Wesley, 1991.

[8] S. L. Ariyavisitakul, J. H. Winters and I. Lee, "Optimum space-time processors with dispersive interference: unified analysis and required filter span", *IEEE Trans. Comm.*, vol. 47, pp. 1073-1083, Jul. 1999.

[9] M. Martone, "An adaptive algorithm for adaptive antenna array low-rank processing in cellular TDMA base-stations", *IEEE Trans. Commun.*, vol. 46, pp. 627-643, May 1998.

[10] M. Martone, "On MMSE Real-Time Antenna Array Processing Using Fourth-Order Statistics in the US Cellular TDMA System", *IEEE Journal Sel. Areas in Comm.*, Vol. 16, N. 8, pp. 1396-1410, Oct. 98.

[11] M. Martone, "Cumulant-based adaptive multi-channel filtering for wireless communication systems with multipath RF propagation using antenna arrays" *IEEE Trans. Veh. Tech.*, Vol. 47, no. 2, pp. 377-391 May 98.

[12] L. Van Trees. *"Detection, Estimation, and Modulation Theory"* Part I, John Wiley 1968.

[13] P.P. Vaidyanathan, *"Multirate Systems and Filter Banks"*, Prentice Hall, 1993.

[14] G. D. Golden, G. J. Foschini, R. A. Valenzuela and P. W. Wolniansky, "Detection algorithms and initial laboratory results using V-BLAST space-time communication architecture", *IEE Electronics Letters*, Vol. 35, N. 1, Jan. 1999.